ELSEVIER

Journal of University of Science and Technology Beijing
Volume 15, Number 2, April 2008, Page 197

Materials

Relationship between texture and residual macro-strain in CVD diamond films based on phenomenological analysis

Weimin Mao[1,2], *Hongxi Zhu*[1], *Leng Chen*[1], *and Huiping Feng*[1]

1) School of Materials Science and Engineering, University of Science and Technology Beijing, Beijing 100083, China
2) State Key Laboratory of Advanced Metals and Materials, University of Science and Technology Beijing, Beijing 100083, China
(Received 2007-04-28)

Abstract: The relationship between texture and elastic properties of chemical vapor deposition (CVD) diamond films was analyzed based on the phenomenological theory, which reveals the influence of crystalline orientation and texture on the residual macro-strain and macro-stress. The phenomenological calculations indicated that the difference in Young's modulus could be 15% in single diamond crystals and 5% in diamond films with homogeneously distributed strong fiber texture. The experimentally measured residual strains of free-standing CVD diamond films were in good agreement with the correspondingly calculated Young's modulus in connection with the multi-fiber textures in the films, though the difference in Young's modulus induced by texture was only around 1%. It is believed that texture should be one of the important factors influencing the residual stress and strain of CVD diamond films.

Key words: diamond films; elastic behavior; texture; residual stresses; chemical vapor deposition (CVD);

[*This work was financially supported by the National Natural Science Foundation of China (No.50372007).*]

1. Introduction

It is known that residual macro-stress exists in chemical vapor deposition (CVD) diamond films very often [1-3], which may lead to poor adhesion of coating films and cracks in free-standing films. Diamond crystal exhibits anisotropic characteristics in its elastic behaviors [4-5]. Therefore, the residual stress level should relate to the grain orientations and textures of the films to a certain extent [4]. Textures have been observed frequently in CVD diamond films depending on the preparation parameters [6-8], and may influence the residual stress directly [9]. Different fiber textures, such as {100}, {110}, {111}, and {221}, were observed in diamond films [10-12]. However, the factors determining the macro-stress are so complicated that it is usually not easy to distinguish the texture effect from other factors. Therefore, it is highly desirable to analyze how far the texture could influence the macro-stress of the CVD diamond films essentially and independently. The problem is discussed in the present study based on the phenomenological theory, in connection with the experimentally measured textures and residual macro-strains of free-standing CVD diamond films.

2. Anisotropic Young's modulus of diamond crystal and its phenomenological analysis

Diamond crystal exhibits obvious elastic anisotropy, of which the Young's modulus reaches the lowest value in <100> and the highest value in <111>, that is, E_{100} and E_{111} are 1050 and 1196 GPa, respectively [4], in which 15% difference in Young's modulus could be observed.

It is known that the phenomenological theory has been widely used to describe the magnetic anisotropy of different magnetic materials. The anisotropy energy of electrical steel with cubic crystal symmetry, for example, can be expressed as a phenomenological function of crystal orientations [13]. The concerned crystal directions [*uvw*] are described in α_1, α_2, and α_3, which are the cosine values of the angles between [*uvw*] and [100], [010], or [001], respectively. The

Corresponding author: Weimin Mao, **E-mail:** wmmao@mater.ustb.edu.cn
Also available online at www.sciencedirect.com

anisotropic Young's modulus E_{uvw} of cubic diamond crystals can be also described based on the same phenomenological theory as

$$E_{uvw} = E_{uvw}(\alpha_1,\alpha_2,\alpha_3) = E_0 + E_1(\alpha_1^2\alpha_2^2 + \alpha_2^2\alpha_3^2 + \alpha_3^2\alpha_1^2) + E_2\alpha_1^2\alpha_2^2\alpha_3^2 + \cdots \approx E_0 + E_1(\alpha_1^2\alpha_2^2 + \alpha_2^2\alpha_3^2 + \alpha_3^2\alpha_1^2) \quad (1)$$

where the first order approximation is chosen, and E_0, E_1, E_2 are the constants characterizing the elastic anisotropy. α_1=1 and α_2=α_3=0 are valid for [100] and α_1=α_2=α_3=$1/\sqrt{3}$ for [111], in which the anisotropy constants can be deduced as E_0=E_{100} and E_1=$3(E_{111}-E_{100})$.

The Young's modulus values of different diamond films vary to a large extent and are strongly dependent on the quality, purity, and deposition technologies [4-5, 14-15]. Therefore, it might be better if the relative Young's modulus e_{uvw} is used instead of E_{uvw}, which is defined according to Eq. (1) as

$$e_{uvw} = e_{uvw}(\alpha_1,\alpha_2,\alpha_3) = \frac{E_{uvw}}{E_0} + \frac{E_1}{E_0}m = 1 + \frac{3(E_{111}-E_{100})}{E_{100}}m = 1 + e_1 m \quad (2)$$

where m= $(\alpha_1^2\alpha_2^2 + \alpha_2^2\alpha_3^2 + \alpha_3^2\alpha_1^2)$ is the orientation factor and e_1 is the relative anisotropy constant.

3. Calculation of the anisotropic Young's modulus

It is imaged for the Young's modulus calculation that the diamond films are located in a coordinate system with *X*, *Y*, and *Z* axes, in which *Z* indicates the normal direction of the diamond films. The grains oriented in the fiber textures {*hkl*} observed in CVD diamond films [10-12], for example, {100}, {011}, {111}, and {122}, have many in-plane directions [*uvw*] with different Young's modulus according to Eq. (2). The relative Young's modulus can be calculated if χ is defined as the rotation angle around the *Z* axis, and the *X* axis at χ=0° is defined as in-plan direction [1 $\bar{1}$ 0], in which the data of single crystal Young's modulus [4] are used. Fig. 1 gives the calculation results, where about 15% fluctuation of Young's modulus is observed. It is to be noticed generally that the {111} or the {100} fiber texture has relatively higher or lower in-plan Young's modulus, respectively.

Different {*hkl*} fiber textures were reported in Refs. [8, 10], in which the {*hkl*} planes of the grains parallel to the film surface, whereas, the <*uvw*> in-plane directions distribute in all film directions homogeneously. Therefore, the average values of the relative Young's modulus $\bar{e}_{hkl}$ concerning the {*hkl*} fiber textures may be useful to classify their different elastic characteristics, which can be calculated as

$$\bar{e}_{hkl} = \frac{\int_0^{\pi/2} e_{uvw}\mathrm{d}\chi}{\pi/2} \quad (3)$$

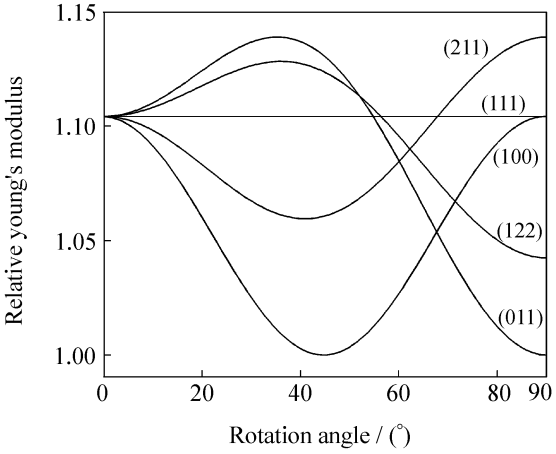

Fig. 1. Calculated relative Young's modulus of different {*hkl*}<*uvw*> orientations.

Table 1 gives the calculated average value of the relative Young's modulus covering all in-plane directions of different {*hkl*} fiber textures. It can be seen that the {111} and the {100} fiber textures possess the highest and lowest average Young's modulus in in-plan directions, that is, 1.104 and 1.052, respectively, where only about 5% difference is obtained.

Table 1. Average value of the relative Young's modulus covering all in-plane directions

(*hkl*)	χ=0 (*X* axis)	χ=π/2 (*Y* axis)	$\bar{e}_{hkl}$
(100)	[0 $\bar{1}$ 1]	[011]	1.052
(011)	[0 $\bar{1}$ 1]	[100]	1.091
(111)	[0 $\bar{1}$ 1]	[$\bar{2}$11]	1.104
(211)	[0 $\bar{1}$ 1]	[$\bar{1}$11]	1.091
(122)	[0 $\bar{1}$ 1]	[$\bar{4}$11]	1.098

Note: $\bar{e}_{hkl}$ —the average value.

4. Measurement of the texture and residual macro-strain in CVD freestanding diamond films

Two freestanding CVD diamond films were prepared by high power DC arc plasma jet operating in gas recycling mode according to Ref. [16], in which the molybdenum substrates were kept at 850°C during diamond deposition. The velocity of the methane flow was 80 mL/min for sample L and 100 mL/min for sample H. The flux of H_2 and Ar was 6.0 and 2.0 L/min, respectively. The film thickness of the samples was about 500 μm. 111, 220, and 311 pole figures were measured in the final grown surface of the dia-

mond films based on the X-ray diffraction technique with a Cu radiation tube, after which the corresponding orientation distribution functions (ODFs) were calculated according to Bunge [17]. Fig. 2 gives the φ_2=45° ODF sections of the diamond samples, which indicates different but rather homogeneously distributed {*hkl*} fiber textures. Sample L has higher {100} and {011} fiber textures, and sample H has higher {111} and {122} fiber textures.

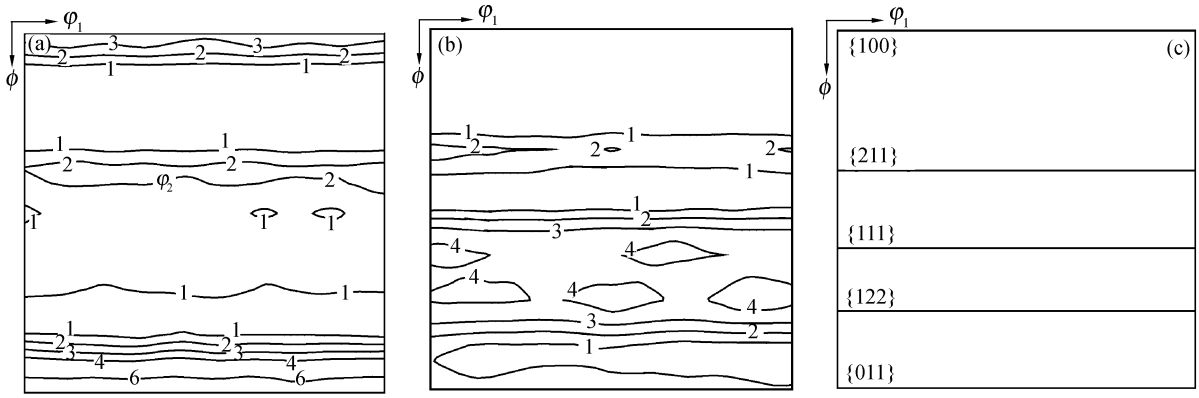

Fig. 2. φ_2=45° ODF sections of the diamond samples (density levels: 1, 2, 3, 4, 6): (a) sample L; (b) sample H; (c) position of {*hkl*} fiber textures in φ_2=45° section.

The X-ray transmission technique with an Mo radiation tube was used to measure the residual elastic normal strains ε in different in-plane directions by changing the χ angles (Fig. 3), in which the elastic change of interplanar space d_{137} was determined. Fig. 4 gives the results of the residual elastic normal strains ε for samples L and H. The residual compressive macro-strains (<0) were observed in general, in which the strain level in sample L is higher than that in sample H. Another characteristic is that the compressive strain trends rising with increasing the χ angle.

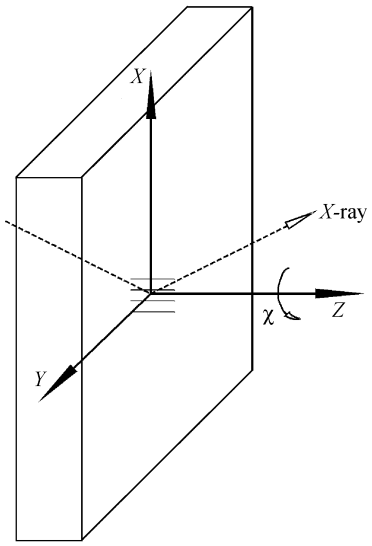

Fig. 3. Sketch map of measuring the residual elastic strains based on the X-ray transmission technique.

5. Calculation of the Young's modulus for polycrystalline diamond films

It is necessary to calculate the average Young's modulus $e(\chi)$ of the polycrystalline diamond films based on the phenomenological theory to analyze the texture effect on the elastic behaviors.

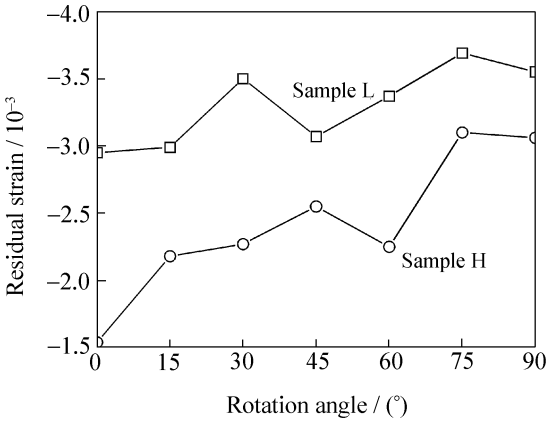

Fig. 4. Residual normal strains (ε) determined in free-standing CVD diamond films.

A set of 936 individual orientations (φ_1, ϕ, φ_2) were taken, which are homogeneously distributed in the orientation space [18]. The ODF values $f(\varphi_1, \phi, \varphi_2)$ on each of the 936 orientations in samples L and H are taken as the weight of the individual orientations. All the 936 orientations and their weights represent the film texture. The average Young's modulus $e(\chi)$ of the diamond film is calculated according to Eq. (2) as

$$\overline{e}(\chi) = \frac{1}{936}\sum_{1}^{936}[f(\varphi_1,\phi,\varphi_2)\cdot e_{uvw}(\alpha_1,\alpha_2,\alpha_3)] \quad (4)$$

where the values α_1, α_2 and α_3 are determined according to Bunge [17] by

$$\begin{cases} \alpha_1 = \cos(\varphi_1+\chi)\cos\varphi_2 - \sin(\varphi_1+\chi)\sin\varphi_2\cos\phi \\ \alpha_2 = -\cos(\varphi_1+\chi)\sin\varphi_2 - \sin(\varphi_1+\chi)\cos\varphi_2\cos\phi \\ \alpha_3 = \sin(\varphi_1+\chi)\sin\phi \end{cases} \quad (5)$$

Fig. 5 gives the calculated average values of the relative Young's modulus for the diamond samples L and H. The relative Young's modulus calculated in sample L is lower than that in sample H, whereas, the Young's modulus decreases with increasing the χ angle. It is worth noticing that the difference of the relative Young's modulus with increasing the χ angle of each sample as well as the difference of that between the two samples is rather low, not more than 1%, despite the difference in textures (Fig. 2).

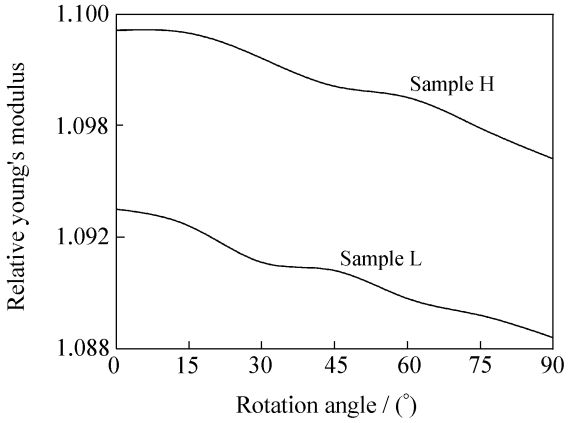

Fig. 5. Calculated average value of the relative Young's modulus for polycrystalline samples.

Both samples L and H exhibit elastic anisotropy, in which, with increasing the χ angle, the residual strain increases and the relative Young's modulus decreases. On the other hand, sample H is of lower elastic strain (Fig. 4) and higher relative Young's modulus (Fig. 5) than sample L. All these phenomena agree with the normal elastic behavior of materials, in which the elastic strain would be reduced under the same residual stress if the Young's modulus becomes higher. Figs. 4 and 5 imply that the difference in Young's modulus induced by texture may be one of the key factors resulting in different elastic strains of samples H and L, though other non-texture factors are not negligible. Around 1% difference in Young's modulus (Fig. 5) might be not very high; however, its influence on residual stress and strain cannot be neglected in consideration of the very high Young's modulus level of diamond crystals in 103 GPa.

6. Summary

The anisotropy of elastic behaviors in diamond crystals and its influence on the macro-strain and stress of CVD diamond films were investigated based on the phenomenological theory. The residual strains of the samples taken from two freestanding CVD diamond films were measured in different in-plan directions, and the relative Young's modulus of the samples were also calculated in connection with the film textures. The theoretical calculations indicated that the difference in Young's modulus could reach 15% in single diamond crystals, 5% in the diamond films with very strong fiber texture, and around 1% in the diamond films with multi-fiber textures. However, the textures of the CVD diamond films could still be one of the important factors influencing residual stress and strain of the films in consideration of the very high Young's modulus level of diamond crystals in 10^3 GPa.

References

[1] C.T. Kuo, C.R. Lin, and H.M. Lien, Origins of the residual stress in CVD diamond films, *Thin Solid Films*, 290-291(1996), p.254.

[2] J.G. Kim and J. Yu, Behavior of residual stress on CVD diamond films, *Mater. Sci. Eng. B*, 57(1998), No.1, p.24.

[3] M. Hempel and M. Härting, Characterization of CVD grown diamond and its residual stress state, *Diamond and Relat. Mater.*, 8(1999), No.8-9, p.1555.

[4] P.J. Gielisse, Mechanical properties of diamond, diamond films, diamond-like carbon and like-diamond material, *Handbook of Industrial Diamonds and Diamond Films*, Eds. by A.P. Mark *et al*., Marcel Dekker, New York, 1998, p.48.

[5] C.A. Klein, Anisotropy of Young's modulus and Poisson's ratio in diamond, *Mater. Res. Bull.*, 27(1992), No.12, p.1407.

[6] H.A. Naseem, M.S. Haque, M.A. Khan, *et al*., High pressure high power microwave plasma chemical vapor deposition of large area diamond films, *Thin Solid Films*, 308-309(1997), p.141.

[7] W.J.P. van Enckevort, G. Janssen, and L.J. Giling, Anisotropy in monocrystalline CVD diamond growth: I. A sphere growth experiment, *J. Crystal Growth*, 113(1991), p.295.

[8] W.M. Mao and N. Chen, Texture analysis of CVD diamond thin films, *J. Univ. Sci. Technol. Beijing* (in Chinese), 22(2000), No.3, p.259.

[9] H. Itoh, S. Lee, K. Sugiyama, *et al*., Adhesion improvement of diamond coating on silicon nitride substrate, *Surf. Coat. Technol.*, 122(1999), No.2-3, p.199.

[10] W.M. Mao, H.X. Zhu, L. Chen, *et al*., Grain orientation dependence on distance to surface of CVD diamond film, *Mater. Sci. Technol.*, 21(2005), No.12, p.1383.

[11] V.M. Ayres, T.R. Bieler, M.G. Kanatzidis, *et al.*, The effect of nitrogen on competitive growth mechanisms of diamond thin films, *Diamond Relat. Mater.*, 9(2000), No.3, p.236.

[12] M.D. Whitfield, J.A. Savage, and R.B. Jackman, Nucleation and growth of diamond films on single crystal and polycrystalline tungsten substrates, *Diamond Relat. Mater.*, 9(2000), No.3, p.268.

[13] J. Szpunar and M. Ojanen, Texture and magnetic properties in Fe-Si steel, *Metall. Trans. A*, 6(1975), p.561.

[14] J. Karner, G. Jörgensen, M. Lahres, *et al*., Non-destructive characterization of CVD diamond films on cemented carbide cutting tools, *Diamond Relat. Mater.*,

7(1998), No.2-5, p.589.

[15] I.B. Yanchuk, M.Y. Valakh, Y. Vul, *et al.*, Raman scattering, AFM and nanoindentation characterization of diamond films obtained by hot filament CVD, *Diamond Relat. Mater.*, 13(2004), No.2, p.266.

[16] F.X. Lü, W.Z. Tang, T.B. Huang, *et al*., Large area high quality diamond film deposition by high power DC arc plasma jet operating at gas recycling mode, *Diamond Relat. Mater.*, 10(2001), No.9, p.1551.

[17] H.J. Bunge, General outline and series expansion method, [in] H.J. Bunge and C. Esling eds. *Quantitative Texture Analysis*, DGM-Informationsgesellschaft, Oberursel, 1981, p.1.

[18] J. Hirsch and K. Lücke, Mechanism of deformation and development of rolling textures in polycrystalline FCC metals, *Acta. Metall*., 36(1988), p.2863.